Hindawi Publishing Corporation
Journal of Nanomaterials
Volume 2015, Article ID 214327, 13 pages
http://dx.doi.org/10.1155/2015/214327

Research Article

Kinetics, Equilibrium, and Thermodynamics of the Sorption of Bisphenol A onto N-CNTs-β-Cyclodextrin and Fe/N-CNTs-β-Cyclodextrin Nanocomposites

Keletso Mphahlele,[1,2] Maurice S. Onyango,[1] and Sabelo D. Mhlanga[3]

[1]*Department of Chemical and Metallurgical Engineering, Tshwane University of Technology, Private Bag X680, Pretoria 0001, South Africa*
[2]*DST-CSIR Nanotechnology Innovation Centre, National Centre for Nanostructured Materials, P.O. Box 395, Pretoria 0001, South Africa*
[3]*Nanotechnology and Water Sustainability Research Unit, College of Science, Engineering and Technology, University of South Africa, Florida, Johannesburg 1709, South Africa*

Correspondence should be addressed to Sabelo D. Mhlanga; mhlansd@unisa.ac.za

Received 18 July 2015; Revised 21 September 2015; Accepted 29 September 2015

Academic Editor: Sesha Srinivasan

We analysed the adsorptive behaviour of Fe/N-CNTs-β-CD nanocomposite in the removal of bisphenol A (BPA) from aqueous solution and identified the key influencing parameters. The Fe/N-CNTs-β-CD nanocomposite adsorbent was prepared by dispersing Fe uniformly on N-CNTs-β-CD using a microwave polyol method and characterized using Fourier transform infrared spectroscopy (FTIR), focused ion beam scanning electron microscopy (FIB-SEM), and energy-dispersive X-ray spectroscopy (EDS). The solution pH and temperature had minimal effect on sorption of BPA while the initial concentration and adsorbent mass affected the adsorption of BPA. No leaching of Fe into the water was observed; thus the nanocomposites were found suitable for use in water purification. From equilibrium isotherm studies, the Langmuir isotherm model gave the best description of the experimental data. The Langmuir monolayer adsorption capacities of BPA onto N-CNTs-β-CD and Fe/N-CNTs-β-CD are 38.20 mg·g^{-1} and 80.65 mg·g^{-1} at 298 K, respectively. Evidently, these adsorption capacity values gave an indication that uniform dispersion of Fe N-CNTs-β-CD prepared by the microwave polyol method enhances the adsorption of BPA. Meanwhile, the sorption kinetics of BPA onto Fe/N-CNTs-β-CD were best described by the pseudo-second-order model.

1. Introduction

Bisphenol A (BPA) is generally used as a monomer in the fabrication of polycarbonates and epoxy resins, as an antioxidant in polyvinyl chloride (PVC) plastics, and as an inhibitor of end polymerization in PVC polymers [1]. As a consequence, BPA is present in products such as the interior coating of wine storage vats, food cans, milk containers, water carboys, food storage vessels, dental materials, baby formula bottles, and water pipes [2]. Due to the recurrent usage of polycarbonate plastics, epoxy resins, and PVC in industry and at homes, BPA has been allegedly observed in rivers, seas, and soils. It is known to have estrogenic activity and it can interfere with endocrine systems of animals and people [3]. Furthermore, BPA is difficult to remove once it builds up in the environment or in the human body due to its poor solubility (381 mg·L^{-1} in water) [4]. The main sources of BPA discharged to environmental water are expected to be the release of industrial wastewater and municipal effluent [5]. Therefore, the removal of BPA from environmental water is necessary and critical.

Some existing technologies to remove BPA from the aquatic environment include adsorption [5–9], solvent extraction [10], membrane separation technology [11], and photodegradation [9, 12]. Removal of BPA by adsorption is economically feasible especially if the adsorbent has high adsorption efficiency and can be recycled. Some adsorbents that have been explored in the removal of BPA from aqueous

solution include activated carbon, mineral clays, raw agricultural solid wastes, and waste materials from forest industries such as maize cob, palm-fruit bunch particles, bagasse pith, sawdust, papaya seeds, and hazelnut shell [13–16]. Most of these materials have low sorption capacity and therefore are not suitable for adsorption technology.

Much attention has shifted towards the use of biopolymers and natural molecules as adsorbents [17]. Cyclodextrins (CDs) are known to form host-guest complexes with hydrophobic compounds. This phenomenon leads to the idea that insolubilized CDs may act as a good adsorbent of BPA [18]. However, because of their solubility in water, CDs cannot be used directly for separation, and hence it seemed plausible that insoluble CDs copolymerized with carbon nanotubes (CNTs) would be good candidates for a recyclable adsorbent [19], which can selectively bind to BPA in water. When CNTs (1–5%) were copolymerized with CDs polymer the recyclability improved considerably, losing only 10% of the polymer mass over twenty-five cycles, compared to 50% loss over nine cycles for the natural CD polymers [20]. In order to further tune CNTs, nitrogen doping is necessary. Modification of the crystalline nanotube properties by controllably placing defects or foreign atoms (heteroatoms) brings along tremendous technological implications [21]. CNTs with nitrogen wall doping possess outer walls with defects and rugosity that provide unique sites for chemical functionalization of the CNTs. This is a way to improve the tube covalent chemistry, which once functionalized can serve to anchor groups or particles that are useful for further functionalization routes [21].

Zero-valent iron (Fe) nanoparticles (NPs) are known for their reductive properties and their sorption capabilities for organics and heavy metals by turning them into less toxic forms or less soluble forms through changes in their oxidation state and/or by adsorption [22]. Concerns over the discharge of these NPs into the environment led to this study where the NPs were anchored on nitrogen doped carbon nanotubes (N-CNTs) in order to immobilize and reduce their environmental mobility. It was believed that a combination of Fe-NPs, N-CNTs, and CD polymers would form an effective adsorbent with enhanced performance for water treatment.

Consequently, the objective of this study was to investigate the sorption equilibrium, kinetics, and thermodynamics of BPA removal from aqueous solution using metal dispersed N-doped carbon nanotubes-β-cyclodextrin (Fe/N-CNTs-β-CD) nanocomposites. The metal nanoparticles were dispersed on N-CNTs by a microwave polyol method. The stability of the metal (Fe) on Fe/N-CNTs-β-CD was explored by determining the amount of Fe released under predetermined sonication times. The effects of time, initial concentration, pH, and temperature on BPA removal from aqueous solution were investigated. Appropriate mathematical models were used to interpret experimental data.

2. Materials and Methods

2.1. Materials. All solvents and chemicals used in this study were purchased from Sigma-Aldrich (USA) and were used as received without further purification. The endocrine disrupting compound (EDC) used as target adsorbate in the present study was bisphenol A (BPA, 97% purity, CAS 80-05-7 and molecular weight of 228.29 g·mol^{-1}). Reagent grade chemicals such as sodium hydroxide (NaOH) and nitric acid (HNO_3, 65%) were used for adjusting initial pH. N,N-Dimethylformamide (DMF, 99% purity) and toluene diisocyanate (TDI, 98% purity) were used to copolymerize β-CDs and N-CNTs.

2.2. Preparation of N-CNTs and Fe/N-CNTs Copolymerized with β-CD. In a typical reaction, 2 g of β-CDs was dried and dissolved in 18 mL of DMF with constant stirring. To this, a solution of presuspended and sonicated (10 min) 1% of N-CNTs and Fe/N-CNTs in 2 mL DMF was added. The mixture of β-CD and Fe/N-CNTs was then heated to 70°C followed by dropwise addition of 2 mL of the bifunctional linker, TDI. This mixture was stirred under inert atmosphere for 24 h. The formed polymer was precipitated, washed with acetone, and dried under vacuum overnight at ambient temperature.

2.3. Batch Adsorption Equilibrium Studies. Batch equilibrium adsorption experiments were carried out using a bottle-point method. In this method a stock solution of BPA (1000 mg·L^{-1}) was prepared and was subsequently diluted to the required initial concentrations. The adsorption capacity of the sorbent towards BPA was determined by contacting a constant mass (0.05 g) of sorbent with a fixed volume (50 mL) in sealed plastic bottles. Two variables were explored: changes in initial pH (pH 2–10) at a fixed concentration of BPA of 100 mg·L^{-1} and changes in temperature (temperatures 298–318 K) at initial concentrations ranging within 10–100 mg·L^{-1} of BPA solution. The bottles were agitated in an isothermal water bath shaker for 24 h until equilibrium was reached.

A calibration curve for BPA was prepared by recording the absorbance values for a range of known concentrations of BPA solution at the maximum absorbance of λ_{max} = 276 nm using double beam Ultraviolet-Visible (UV-Vis) spectrophotometer (Lambda 7505, Perkin Elmer). The amount of BPA adsorbed onto sorbent, q_e (mg·g^{-1}), was calculated by the following equation:

$$q_e = \frac{(C_o - C_e)\,V}{m}, \tag{1}$$

where C_o and C_e are the initial and equilibrium concentrations of BPA solution (mg·L^{-1}), respectively, V is the total volume of the BPA solution (L), and m is the mass of sorbent used (g).

Further, two equilibrium isotherm models, the Langmuir and Freundlich models, were used to describe the relationship between the adsorbed amount of BPA and its equilibrium concentration in solution. The Langmuir isotherm is represented:

$$q_e = \frac{Q_{max} b_L C_e}{1 + b_L C_e}. \tag{2}$$

The linearized Langmuir isotherm is expressed by

$$\frac{C_e}{q_e} = \frac{1}{b_L Q_{max}} + \frac{C_e}{Q_{max}}, \tag{3}$$

where b_L is the Langmuir affinity constant ($L \cdot mg^{-1}$) and Q_{max} is the maximum adsorption capacity of the material ($mg \cdot g^{-1}$).

The Freundlich isotherm is represented by the following [23]:

$$q_e = K_F C_e^{1/n}. \quad (4)$$

The linearized Freundlich isotherm is expressed as follows:

$$\ln q_e = \ln K_F + \frac{1}{n} \ln C_e, \quad (5)$$

where K_F is the Freundlich constant ($L \cdot g^{-1}$) and n is the heterogeneity factor. The K_F value is related to the adsorption capacity, while $1/n$ value is related to the adsorption intensity. The magnitude of exponent (n) gives an indication of the favourability of the sorbent/sorbate system [24].

2.4. Batch Adsorption Kinetics. The kinetics of BPA removal from aqueous solution were studied by varying mass of the sorption media and initial concentration of BPA. The experiments were carried out separately in 1 L batch reactor. When exploring the effect of mass (0.5 g, 0.7 g, and 1 g) of sorption media, the initial BPA concentration of 50 $mg \cdot L^{-1}$ was used. In the case when initial (50, 75, and 100 $mg \cdot L^{-1}$) concentration was a variable, the sorbent mass was fixed at 1 $g \cdot L^{-1}$. The reactor was stirred with an overhead stirrer operated at 200 rpm. At predetermined time intervals, 5 mL samples were taken from the reactor and filtered through a syringe filter and residual BPA concentration was analysed by UV-Vis spectroscopy. By performing appropriate material balance, the quantity of BPA adsorbed at the selected time intervals was determined and used for kinetic analysis. The amount of BPA adsorbed at any time was calculated by

$$q_t = \frac{(C_o - C_t) V}{m}, \quad (6)$$

where C_t is the concentration of BPA solution at any time ($mg \cdot L^{-1}$). The kinetic data was modelled using the pseudo-first-order, pseudo-second-order, and Elovich kinetic models. The Lagergren pseudo-first-order kinetic rate expression is given by [24, 25]:

$$\frac{dq_t}{dt} = k_1 (q_e - q_t). \quad (7)$$

Integrating this for the boundary conditions $t = 0$ to $t = t$ and $q_t = 0$ to $q_t = q_t$, (7) may be rearranged for linearized data plotting as shown in

$$\log (q_e - q_t) = \log q_e - \frac{k_1}{2.303} t, \quad (8)$$

where k_1 is the rate constant of first-order sorption (min^{-1}). The pseudo-second-order kinetic rate equation is expressed as [15]:

$$\frac{dq_t}{dt} = k_2 (q_e - q_t)^2. \quad (9)$$

Integrating this for the boundary conditions $t = 0$ to $t = t$ and $q_t = 0$ to $q_t = q_t$, (9) may be rearranged for linearized data plotting as

$$\frac{t}{q_t} = \frac{1}{k_2 q_e^2} + \frac{t}{q_e}, \quad (10)$$

where k_2 is the rate constant of second-order sorption ($g \cdot mg^{-1} \cdot min^{-1}$). Finally, the Elovich model equation is generally expressed as [26]:

$$\frac{dq_t}{dt} = \alpha \exp(-\beta q_t), \quad (11)$$

where α is the initial adsorption rate ($mg \cdot g^{-1} \cdot min^{-1}$) and β is the desorption constant ($g \cdot mg^{-1}$). To simplify the Elovich equation, it can be assumed that $\alpha\beta t \gg t$ and by applying the boundary condition $q_t = 0$ at $t = 0$ and $q_t = q_t$ at $t = t$, (11) becomes

$$q_t = \frac{\ln(\alpha\beta)}{\beta} + \frac{1}{\beta} \ln t. \quad (12)$$

2.5. Error Analysis. Due to the inherent bias resulting from linearization [27], attempts were made to compare the kinetic and equilibrium models by the square sum of errors (SSE). SSE is represented by

$$\text{SSE} = \sum_{i=1}^{n} \frac{\sqrt{(q_{e,\text{exp}} - q_{e,\text{cal}})^2}}{N}. \quad (13)$$

3. Results and Discussion

3.1. Characterization of the Nanocomposite Materials before and after Sorption. For most real-world applications, experimental conditions need to be tightly controlled in order to obtain nanoparticles (NPs) with at least the following characteristics: identical particles in terms of size (a uniform size distribution), shape, or morphology, chemical composition and crystal structure (ideally, core and surface composition must be the same, unless specifically designed for other purposes), and monodispersity (no aggregation) [28, 29]. A facile, fast, and green microwave polyol approach was adopted to disperse Fe nanoparticles into the internal matrix of N-CNTs. The sorbent was characterized before and after BPA sorption and the results are as discussed in Sections 3.1.1 and 3.1.2.

3.1.1. Focused Ion Beam Scanning Electron Microscopy (FIB-SEM). The surface morphology of the Fe/N-CNTs-β-CD sorbent before and after sorption of BPA is shown in Figure 1. The FIB-SEM was used to assess the morphological changes in the sorbent surface following sorption of BPA. The sorbent before sorption exhibited a cave-like, irregular, and uneven surface morphology. The roughness of the surface is considered as a factor providing an increase in the surface area. In addition, the material was porous and this property reduces the diffusional resistance and makes it easy for mass transfer

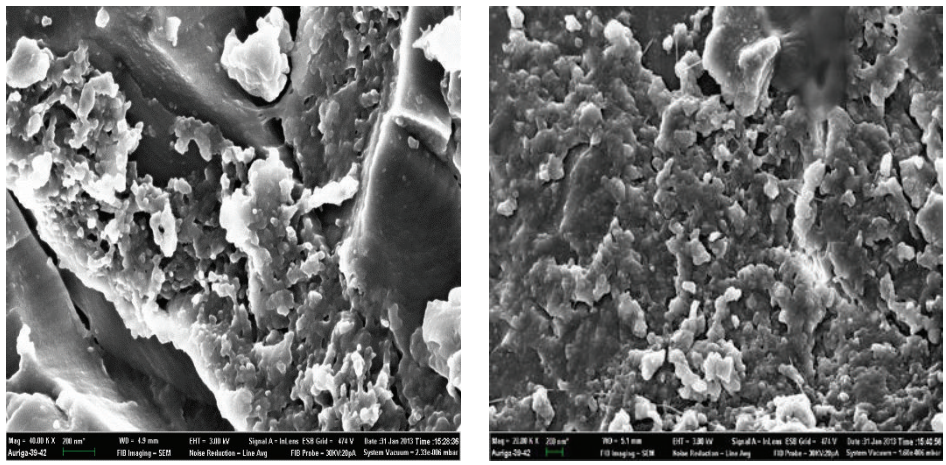

(a) (b)

Figure 1: SEM images of Fe/N-CNTs-β-CD nanocomposite polymer before (a) and after (b) adsorption of BPA. The Fe/CNTs could not be seen because they were embedded in the bulk of the β-CD polymer.

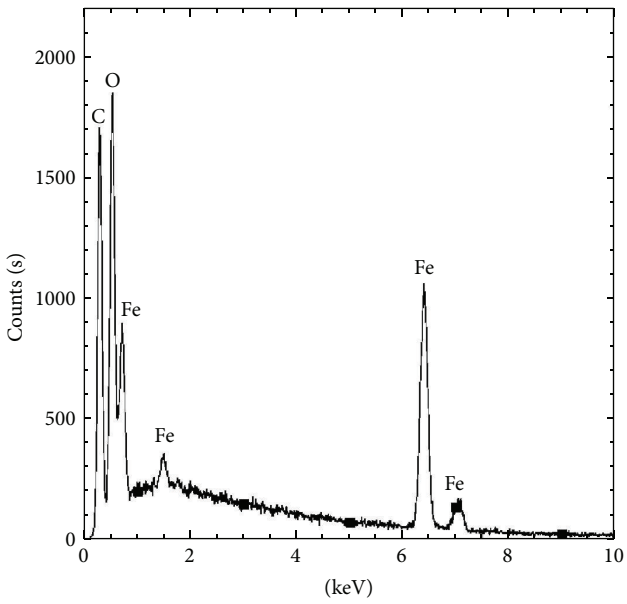

Figure 2: Energy-dispersive X-ray spectroscopy of Fe/N-CNTs.

to take place because of high internal surface area [30, 31]. It is clearly seen that, after sorption process (Figure 1(b)), the pores and surface of the sorbent were covered; the sorbate may have densely and homogeneously adhered to the surface of the sorbent as a result of either natural entrapment into the porous nanocomposite due to physical sorption by electrostatic forces or covalent binding between the cellular sorbent and the sorbate [32, 33].

Figure 2 shows the EDS analysis of the Fe/N-CNTs nanocomposites taken from various points with high magnification in order to do an elemental qualitative composition of the metal particles. The nanocomposites contained the Fe as desired. The EDS analysis gave quantitative results of Fe

Table 1: Quantitative results for Fe/N-CNTs using EDS.

Element line	Weight percentage	Weight % error	Atom %	Atom % error
C K	19.43	±0.17	31.5	±0.24
O K	60.55	—	65.1	±23.25
Fe K	20.01	±6.34	3.4	±0.11
Total	100		100	

at concentrations above 20 wt.%. Accuracies for the major elements in aqueous standards were 6.34% (Table 1).

3.1.2. FTIR Spectroscopy Analysis. Sorbents are widely used as separation media in water treatment to remove organic and inorganic contaminants from polluted water. Nanomaterials have two main properties that make them particularly attractive as sorbents. On a mass basis, they have greatly larger surface areas than their bulk counterparts. Nanomaterials can also be functionalized with various chemical groups to increase their affinity towards the targeted contaminants [34]. Concerns over the discharge of these nanomaterials into the environment prompted us to use N-CNTs as a support for Fe nanoparticles in order to immobilize and reduce their environmental mobility [20]. CDs are slightly soluble in water and this restricts their application in water purification. This necessitates their functionalization and, in particular, polymerization of the parental CDs with suitable bifunctional linkers such as hexamethylene diisocyanate (HDI) and toluene diisocyanate (TDI) [35]. Evidence of polymerization was confirmed by the disappearance of the isocyanate peak (Figure 3(a)) in the FTIR spectrum. Complete disappearance of the isocyanate peak was observed after 16 h of polymerization (Figure 3(b)). This was an indication that polymerization was complete. The FTIR bands corresponding to C-H (2938 cm^{-1}), C=O (1714 cm^{-1}), and C=C (1631 cm^{-1}) further confirmed that polymerization between monomers (N-CNTs

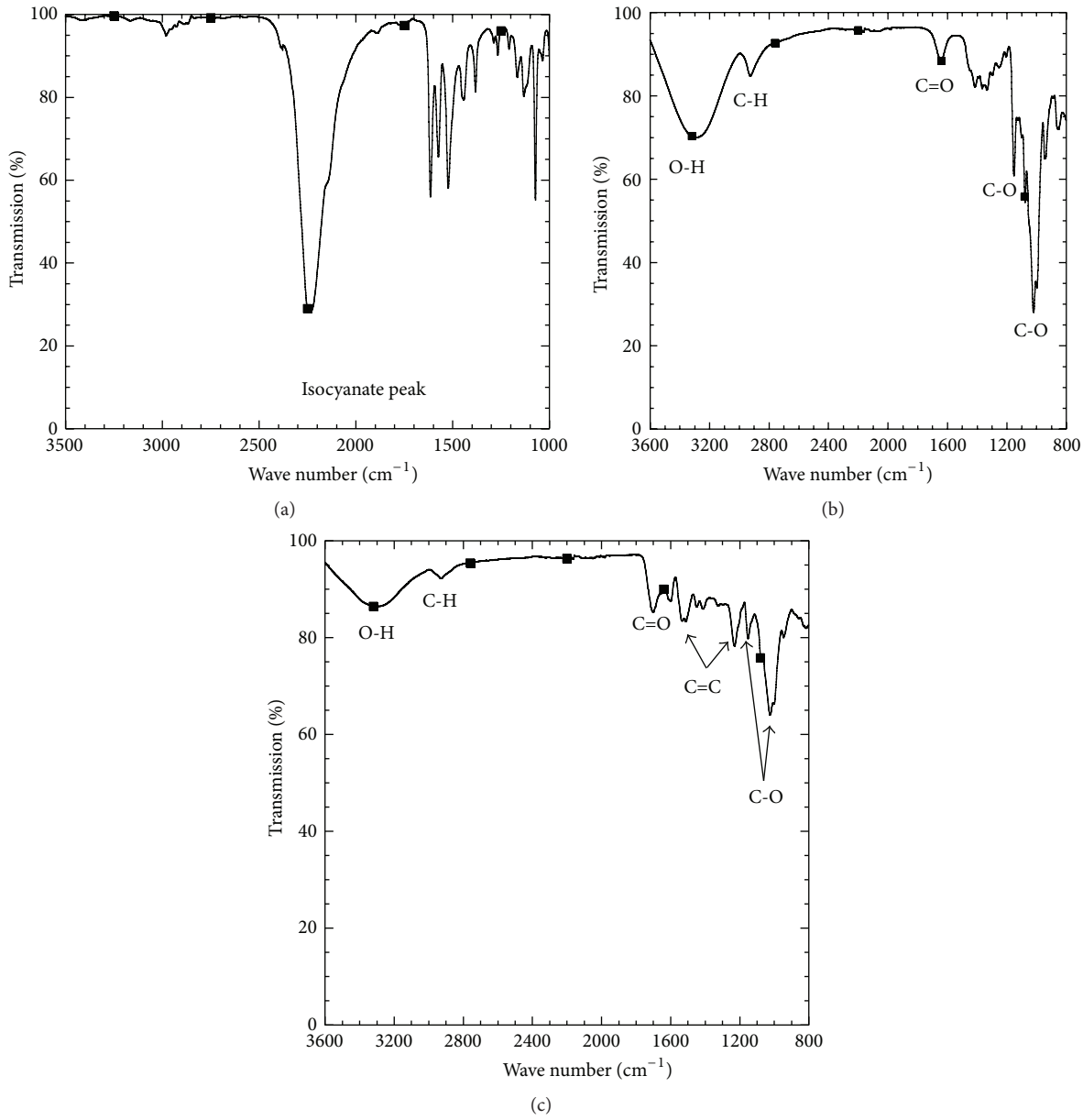

Figure 3: FTIR spectra of the copolymerization of β-CD and metal/N-CNTs: (a) at start of the reaction, (b) after 16 h, and (c) after adsorption.

and β-CD) and the linker (TDI) had occurred [36, 37]. Comparing Figures 3(b) and 3(c) after adsorption, a shift or disappearance of peaks C-O (1200 cm^{-1} and 1000 cm^{-1}) and C-H (2938 cm^{-1}) was observed. The appearance of new peaks was also observed, that is, C=C at 1600 cm^{-1} and 1500 cm^{-1}. These changes observed in the spectrum indicate the possible involvement of those functional groups on the surface of the sorbent during sorption process.

3.2. Effect of pH on BPA Sorption. The pH of water varies for different sources. From a chemistry point of view, this affects the charge of a given sorbate and the surface charge density of the sorbent. Thus depending on the pH value of solution and nature of the sorption process, a coulombic repulsive or attractive force may be experienced in a sorptive system [9, 38]. The effect of solution pH on BPA sorption onto CNTs-β-CD and Fe/N-CNTs-β-CD was studied by varying the initial pH from 2 to 12. The results are presented in Figure 4. The removal of BPA from aqueous solution was found to be insensitive to pH changes. It is well known that CDs form host-guest complexes with hydrophobic compounds [18]. These results suggested that BPA was trapped by the sorbents through the hydrophobic interaction and the hydrogen-bonding interaction simultaneously [39]. A pH 7 was selected for the following studies to minimise cost of pH adjustment that may be required in real field situation. Meanwhile, it was also observed that the sorption capacity for sorbent Fe/N-CNTs-β-CD was higher than that of N-CNTs-β-CD, that is, 79.85 mg·g^{-1} and 38.9 mg·g^{-1}, respectively. Having Fe nanoparticles on the surface of the N-CNTs

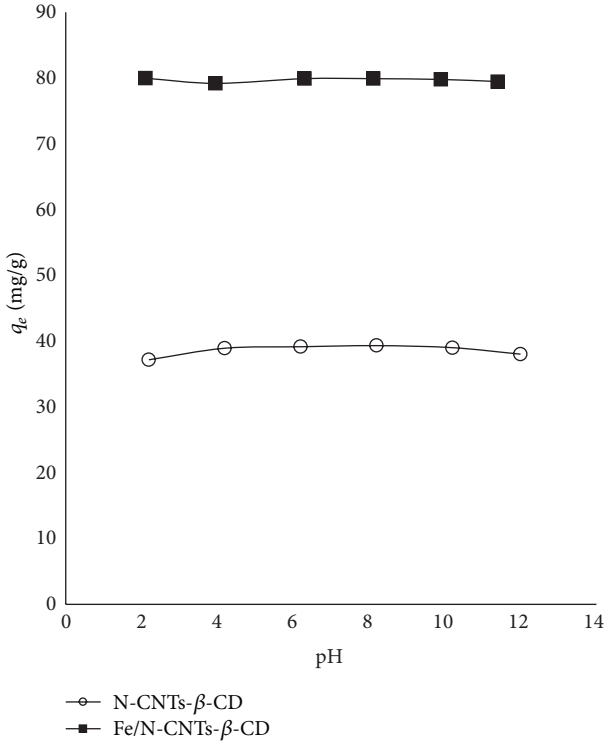

Figure 4: The effect of pH on the removal of BPA.

enhanced the sorption capacity of the sorbent. Consequently the subsequent discussions are centred on Fe dispersed N-CNTs-β-CD.

3.3. Effect of Temperature: Sorption Equilibrium Isotherms. The effect of temperature on sorption capacity was investigated in the temperature range of 298 K to 318 K. The interaction between N-CNTs-β-CD and Fe/N-CNTs-β-CD with BPA is presented in the form of equilibrium data (experimental data) (Figures 5 and 6). The experimental data show that sorption capacity of BPA is insensitive to temperature. The temperature range used did not cause any effect simply because the temperature difference was not large. Environmental water sources do not have temperatures beyond 318 K. As such, it was not worthwhile to carry out the sorption studies beyond this temperature. In Figure 5(a), a rectangular type isotherm was observed in which the curve rose sharply in the initial stages, demonstrating that there was an abundance of readily available sites. This was followed by an asymptotic plateau indicating that the sorbent was now saturated, that is, formation of monolayer. In the presence of Fe in the nanocomposite, the rate of BPA sorption was much faster (Figure 6(a)).

Solid-liquid equilibrium can be easily described by sorption isotherms. To model the isotherm data, the Langmuir and Freundlich models are often used. From (3) linear curves were obtained by plotting C_e/q_e versus C_e for the Langmuir isotherm and $\ln C_e$ versus $\ln q_e$ for the Freundlich isotherm. The plots of C_e/q_e versus C_e are used to determine Langmuir parameters. The data fit quite well to the Langmuir model for the Fe/N-CNTs-β-CD nanocomposites as all R^2 values were 1.000. $Q_{\max}$ was 80.65 mg·g^{-1} for Fe/N-CNTs-β-CD and was independent of temperature. The Freundlich isotherm plots are presented in Figures 5(c) and 6(c). It was also observed that data fitted fairly well. From the plots, the Langmuir and Freundlich isotherm parameters are summarized in Table 2. There was a minor change in the Freundlich isotherm parameters with a change in temperature.

Linear regression has been developed as the most important option in designing sorption systems but may produce inconsistency (between the predictions and experimental data). Depending on the way adsorptive equation is linearized, the error distribution changes can worsen. This has attested the utilization of nonlinearized models in conjunction with number of error analysis techniques [27, 40]. A comparison of SSE for the two isotherms is also listed in Table 2. From the SSE values, the Langmuir isotherm was the most suitable for the experimental data compared to the Freundlich isotherm.

3.4. Adsorption Kinetics

3.4.1. Effect of Mass. Figure 7 shows the uptake-time plots for the study of the effect of the mass of Fe/N-CNTs-β-CD use on sorption kinetics. The uptake of BPA was rapid and dependent on the mass of the sorbent. The rapid rate of the sorption was attributed to the size of the particles. In sorption, sorbent particle size affects the kinetics of uptake since as particle size changes, also the diffusion path changes. Small particles exhibit faster sorption kinetics due to reduced diffusional path or resistance. The kinetic data presented in Figure 7(a) were further modelled using pseudo-first-order, pseudo-second-order, and Elovich models in an attempt to extract model parameters and to determine which model offers the best description of the data. The data fitting to the linearized pseudo-first-order model (8) is presented in Figure 7(b). Linear curves were obtained only up to the 60th minute, beyond which the curves became nonlinear (this part is not shown in Figure 7(b)) suggesting that this model did not sufficiently describe the experimental data. Figure 7(c) shows the data fitted to the linear form of the pseudo-second-order model (10). Evidently, the correlation between the experimental data over the time period and the theoretical data was good for this model. All the correlation coefficients, R^2, were >0.99. For the Elovich model, the experimental data fitted to the linear form (12) is summarized in Figure 7(d). Similar to the case of the pseudo-first-order model, linear curves were only obtained up to the 60th minute.

The model parameter values are summarized in Table 3. The parameters depend on sorbent mass. For instance, the k_2 value increased with an increase in sorbent mass. This was due to the fact that the BPA concentration in the solution was rapidly reduced as mass of sorbent was increased. The mass of the sorbent is related to the number of active sites for sorption and both of these increase in parallel [41]. The active sites determine the extent and rate of sorption. Furthermore, the SSE was used to determine the best fit model since linear regression has some inherent weakness. Minimum SSE for

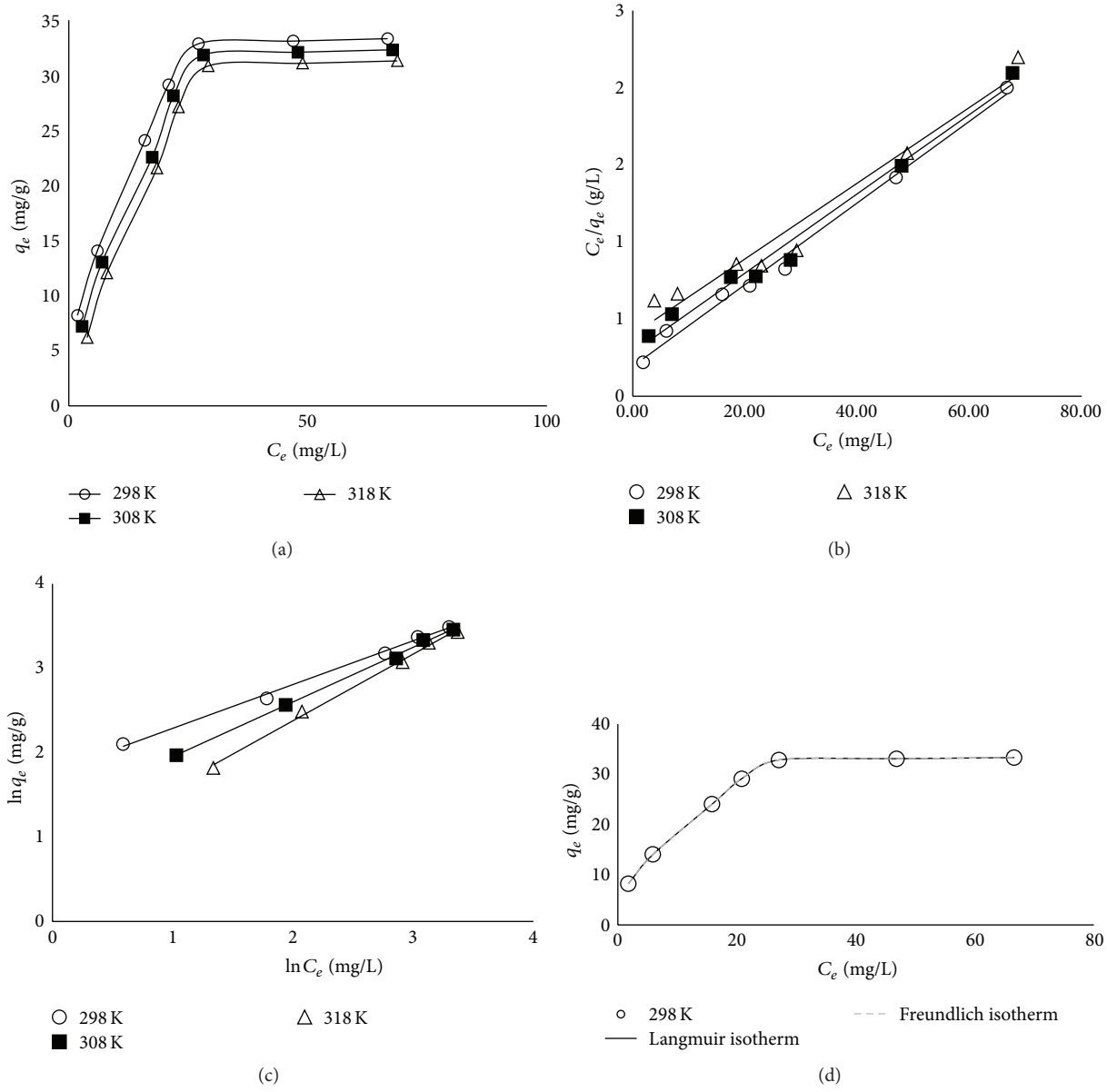

Figure 5: (a) Adsorption isotherm of BPA in aqueous solution (1), (b) linearized Langmuir isotherm (3) for BPA adsorption, (c) linearized Freundlich isotherm (5) at temperatures 298 K, 308 K, and 318 K, and (d) Langmuir and Freundlich isotherms ((2) and (4), resp.) obtained using nonlinear fitting onto N-CNTs-β-CD at 298 K. Sorbent dose = 0.05 g/50 mL solution.

Table 2: Langmuir and Freundlich isotherm parameters at three temperatures for the sorption of BPA by N-CNTs-β-CD and Fe/N-CNTs-β-CD.

	Langmuir				Freundlich			
Temperature (K)	Q_{max} (mg/g)	b_L (L/mg)	R^2	SSE	K_F	n	R^2	%SSE
N-CNTs-β-CD								
298	38.20	0.12	0.98	0.00	6.80	2.40	0.94	0.001
308	39.40	0.08	0.97	0.00	6.80	2.00	0.92	0.000
318	41.50	0.06	0.95	0.00	3.40	1.70	0.90	0.000
Fe/N-CNTs-β-CD								
298	80.65	11.27	1.00	0.00	102.82	2.26	0.99	0.001
308	80.65	9.54	1.00	0.00	116.08	1.92	0.98	0.006
318	80.65	8.86	1.00	0.00	125.67	1.73	0.97	0.006

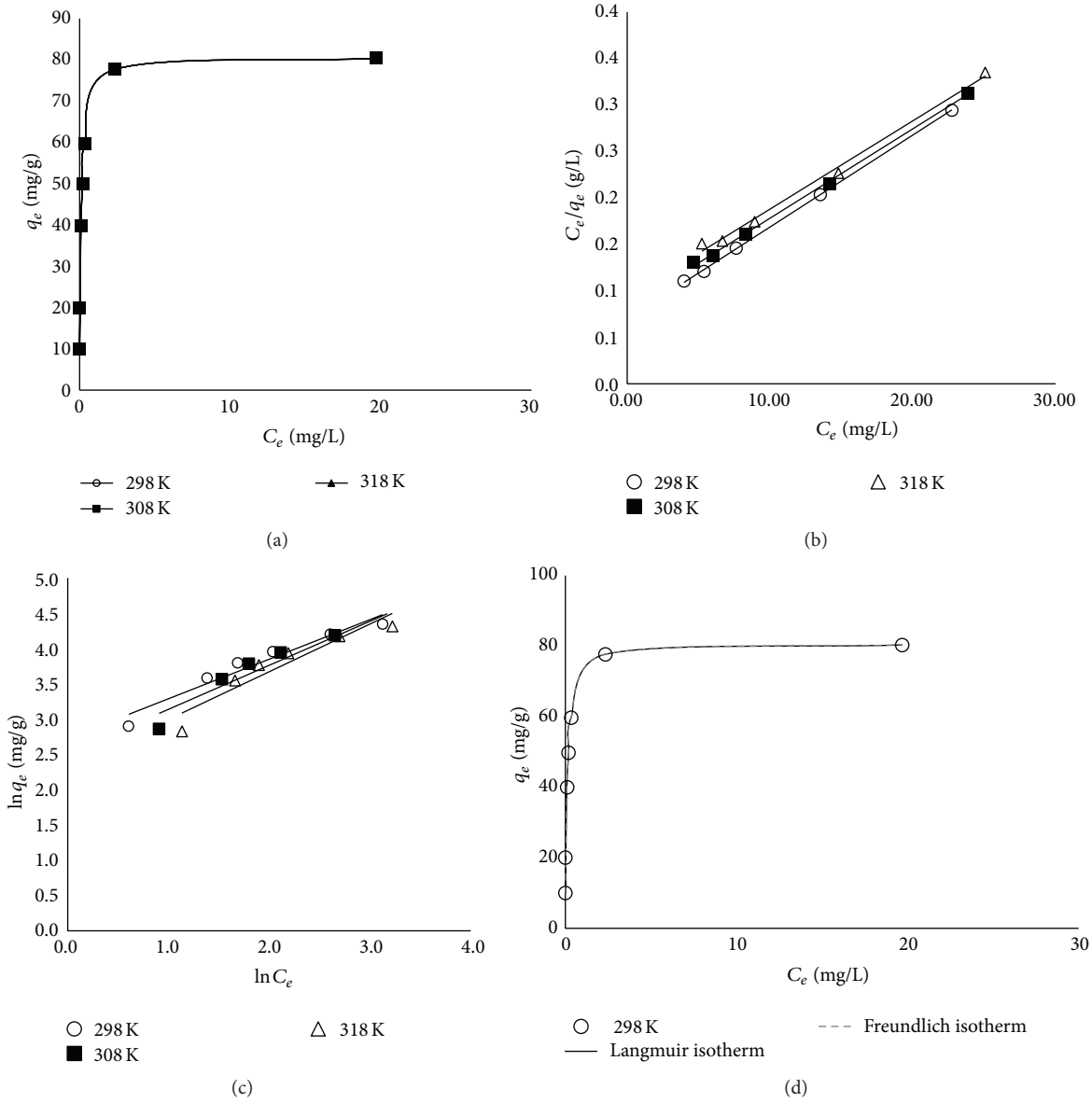

Figure 6: (a) Adsorption isotherm of BPA in aqueous solution (1), (b) linearized Langmuir isotherm (3) for BPA adsorption, (c) linearized Freundlich isotherm (5) at temperatures 298 K, 308 K, and 318 K, and (d) Langmuir and Freundlich isotherms ((2) and (4), resp.) obtained using nonlinear fitting onto Fe/N-CNTs-β-CD at 298 K. Sorbent dose = 0.05 g/50 mL solution.

the sorption of BPA onto Fe/N-CNTs-β-CD was obtained for the pseudo-second-order model.

3.4.2. Effect of Initial Concentration. The kinetics of BPA uptake for various initial concentrations are shown in Figure 8(a). The uptake of BPA was fast in the first 60 min, after which equilibrium was achieved for all the BPA initial concentrations used. Compared with bulk activated carbon reported by Li et al. [8], the kinetic performance of Fe/N-CNTs-β-CD in BPA uptake was much faster. As already discussed in Section 3.4.1, the nanomaterials resulted in reduced resistance to mass transfer and increased surface area, hence the faster uptake of BPA seen in this study. Generally, the uptake of BPA increased with an increase in initial concentration. The sorption of BPA is a passive process driven by concentration gradient as a driving force. The higher the initial concentration, the higher the driving force leading to a higher uptake rate [42, 43].

The kinetic data was further fitted to the linear forms of the pseudo-first-order, pseudo-second-order, and Elovich model at different initial BPA concentrations. The modelling plots are given in Figures 8(b), 8(c), and 8(d). The pseudo-first-order and Elovich models plots were only linear up to the 60th min (nonlinear section omitted). The pseudo-second-order model gave a good fit over the entire sorption period. The extracted model parameters are summarized in Table 4. Overall, the model parameters were dependent on the initial concentration of BPA although no trend was visible. Whereas

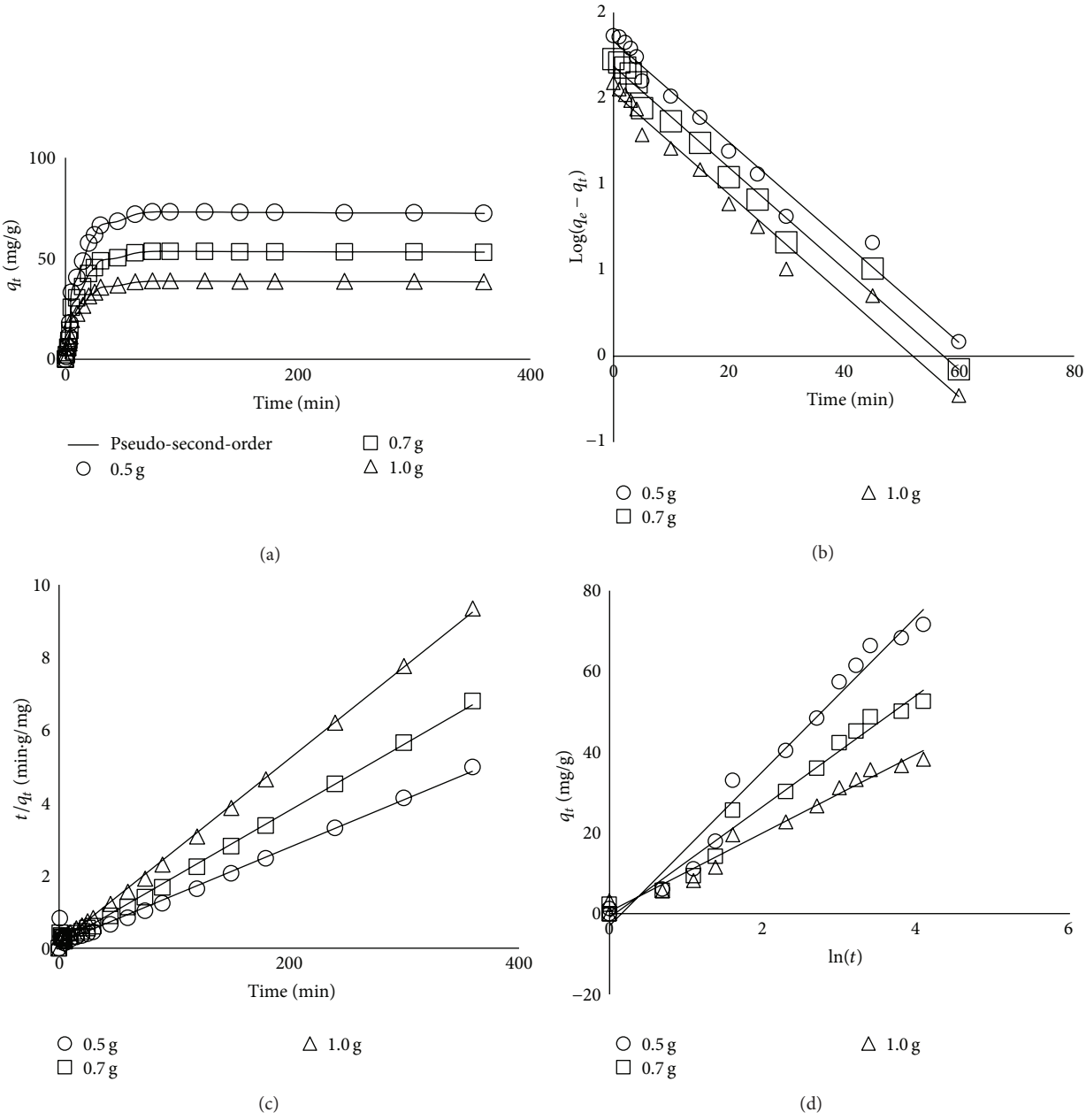

Figure 7: The influence contact time on the sorption capacity of BPA for different mass of Fe/N-CNTs-β-CD: (a) nonlinear fitting of pseudo-second-order model, (b) linearized pseudo-first-order kinetic model (8), (c) linearized pseudo-second-order kinetic model (10), and (d) linearized Elovich model (12) obtained at 298 K, 1000 mL solution.

Table 3: Pseudo-first-order, pseudo-second-order, and Elovich kinetic models parameters at 298 K, with an initial concentration of 50 mg·L^{-1} and volume of 1000 mL for Fe/N-CNTs-β-CD with different masses: 0.5 g, 0.7 g, and 1.0 g.

Fe/N-CNTs-β-CD													
Mass (g)	$q_{e,exp}$ (mg·g^{-1})	Pseudo-first-order kinetic model				Pseudo-second-order kinetic model				Elovich kinetic model			
		K_1 (1/min)	$q_{e,cal}$ (mg·g^{-1})	R^2	SSE	K_2 (g/mg·min)	$q_{e,cal}$ (mg·g^{-1})	R^2	SSE*	α (mg/g·min)	β	R^2	SSE
0.50	72.90	0.067	67.87	0.98	14.00	0.001	76.34	0.99	7.01	16.33	0.05	0.98	7.11
0.70	53.40	0.067	47.97	0.98	18.01	0.002	54.64	1.00	12.00	12.78	0.07	0.98	16.95
1.00	38.90	0.068	34.08	0.98	10.99	0.004	39.52	1.00	4.97	10.24	0.10	0.98	5.00

*Values represent the minimum sum of square error (SSE).

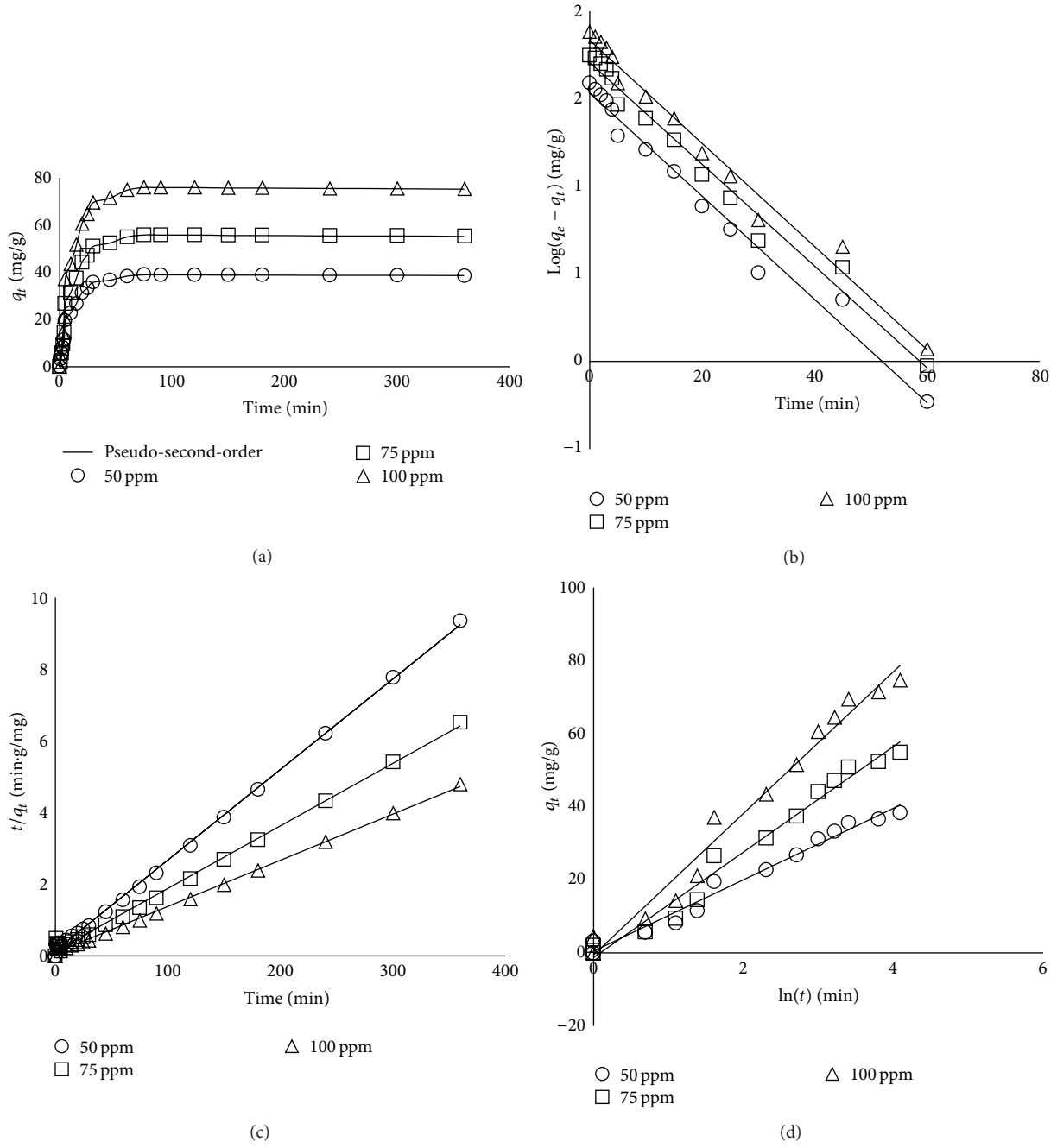

Figure 8: The influence contact time on the sorption capacity of BPA for different concentrations of Fe/N-CNTs-β-CD: (a) nonlinear fitting of pseudo-second-order model, (b) linearized pseudo-first-order kinetic model (8), (c) linearized pseudo-second-order kinetic model (10), and (d) linearized Elovich model (12) obtained at 298 K, 1000 mL solution.

Table 4: Pseudo-first-order, pseudo-second-order, and Elovich kinetic models parameters at 298 K for Fe/N-CNTs-β-CD at different concentrations of BPA: 50 mg·L^{-1}, 75 mg·L^{-1}, and 100 mg·L^{-1}. Sorbent dose = 1 g/1000 mL solution.

Fe/N-CNTs-β-CD													
C_o (ppm)	$q_{e,\exp}$ (mg·g^{-1})	Pseudo-first-order kinetic model				Pseudo-second-order kinetic model				Elovich kinetic model			
		K_1 (1/min)	$q_{e,\text{cal}}$ (mg·g^{-1})	R^2	SSE	K_2 (g/mg·min)	$q_{e,\text{cal}}$ (mg·g^{-1})	R^2	SSE*	α (mg/g·min)	β	R^2	SSE
50	38.90	0.007	34.08	0.98	15.80	0.004	39.52	1.00	4.97	10.24	0.10	0.98	5.00
75	55.80	0.007	50.71	0.98	5.00	0.002	55.18	1.00	8.00	10.15	0.07	0.98	8.11
100	75.90	0.007	68.02	0.98	7.00	0.002	77.52	1.00	8.99	18.82	0.05	0.98	8.99

*Values represent the minimum sum of square error (SSE).

Table 5: Thermodynamic parameters for the sorption of BPA at different temperatures by N-CNTs-β-CD and Fe/N-CNTs-β-CD adsorbents.

	ΔH° (kJ·mol^{-1})	ΔS° (J/mol·K)	ΔG° (kJ·mol^{-1})		
Sorbent			298 K	308 K	318 K
N-CNTs-β-CD	−40.92	−125.00	−3.65	−2.48	−1.15
Fe/N-CNTs-β-CD	−1.33	41.60	−13.73	−14.15	−14.15

the pseudo-second-order model provided a fair prediction of the experimental uptake values ($q_{e,\text{exp.}}$), the equilibrium uptake values predicted by the pseudo-first-order model were relatively low. This indicated that the pseudo-first-order model did not describe the BPA-Fe/N-CNTs-β-CD interaction. From the linear regression coefficients and SSE values, it could be concluded that both the pseudo-second-order and Elovich models gave a satisfactory description of experimental data.

3.5. Sorption Thermodynamics. A thermodynamic consideration of sorption processes is essential to determine whether the process is spontaneous or not. Gibbs's free energy change, ΔG°, is the essential measure of spontaneity [44]. A reaction occurs spontaneously at a given temperature if ΔG° is a negative value. The thermodynamic parameters of Gibb's free energy change, ΔG°, enthalpy change, ΔH°, and entropy change, ΔS°, for the adsorption processes were calculated using the equations below:

$$\begin{aligned} \Delta G^\circ &= -RT \ln K_a, \\ \Delta G^\circ &= \Delta H^\circ - T\Delta S^\circ, \end{aligned} \tag{14}$$

where R is universal gas constant (8.314 J·mol^{-1}·K^{-1}) and T is the absolute temperature in K.

A positive value of enthalpy change shows that the process is endothermic, while a negative value indicates an exothermic process. A plot of $\ln K_L$ against $1/T$ should yield a straight line with the intercept of $\Delta S^\circ/RT$ and a slope of $\Delta H^\circ/R$ [45]. The thermodynamic parameters are given in Table 5. The negative values of Gibb's free energy change confirmed the feasibility of the process and indicate the spontaneous nature of sorption of BPA at all the temperatures of all the sorbents studied. The values of ΔG° decreased from −3.65 kJ·mol^{-1} to −1.15 kJ·mol^{-1} for adsorbents N-CNTs-β-CD and increased from −13.73 kJ·mol^{-1} to −14.15 kJ·mol^{-1} for Fe/N-CNTs-β-CD, indicating that the sorption of BPA on Fe/N-CNTs-β-CD is feasible and spontaneous. The negative value of ΔH°, −40.92 kJ·mol^{-1} and −1.33 kJ·mol^{-1} onto N-CNTs-β-CD and Fe/N-CNTs-β-CD, respectively, indicated that the sorption process was exothermic. The negative value of ΔS° for N-CNTs-β-CD indicated a decreased randomness at the solid-solute interface during sorption process possibly due to the rapid saturation of the active sites of these materials, while the positive value of ΔS° for Fe/N-CNTs-β-CD indicated an increased randomness at the solid-solute interface during adsorption process.

4. Conclusions

Stable N-CNTs-β-CD and Fe/N-CNTs-β-CD nanocomposites were successfully prepared and evaluated as sorbents for the removal of BPA from aqueous solution under varying process conditions. The results revealed that dispersing metal nanoparticles onto N-CNTs-β-CD significantly enhances the BPA sorption capacity. From equilibrium studies, it has been shown that the Langmuir isotherm model gives a good description of experimental data for the metal nanoparticles dispersed N-CNTs-β-CD composite, that is, Fe/N-CNTs-β-CD. Further, the Langmuir monolayer capacity of Fe/N-CNTs-β-CD was 80.65 mg·g^{-1} at all temperatures. This value is competitive when compared to those reported in open literature. Meanwhile, from the kinetic studies, the uptake of BPA by Fe/N-CNTs-β-CD composite was rapid and followed the pseudo-second-order model. The results obtained thus far give an indication that Fe/N-CNTs-β-CD nanocomposites are a potential sorbent for water treatment applications. Further work is however needed to evaluate the long term stability of the materials and to get some indication of cost, and reusability of the material needs to be evaluated in adsorption-desorption studies.

Conflict of Interests

The authors declare that there is no conflict of interests regarding the publication of this paper.

Acknowledgments

The authors wish to thank the National Research Foundation of South Africa (NRF, SA) under the Nanotechnology Flagship Programme (UID 68705) and the Tshwane University of Technology and the Council for Scientific and Industrial Research (CSIR, Pretoria) for financial support. Sabelo D. Mhlanga is grateful to Dr. D. Saad for her various contributions during preparation of the paper.

References

[1] G. Xiao, L. Fu, and A. Li, "Enhanced adsorption of bisphenol A from water by acetylaniline modified hyper-cross-linked polymeric adsorbent: effect of the cross-linked bridge," *Chemical Engineering Journal*, vol. 191, pp. 171–176, 2012.

[2] A. M. Soto, L. N. Vandenberg, M. V. Maffini, and C. Sonnenschein, "Does breast cancer start in the womb?" *Basic & Clinical Pharmacology & Toxicology*, vol. 102, no. 2, pp. 125–133, 2008.

[3] H. Maruyama, H. Seki, Y. Matsukawa, A. Suzuki, and N. Inoue, "Adsorption behavior of bisphenol-A and diethyl phthalate onto bubble surface in nonfoaming adsorptive bubble separation," *Chemical Engineering Journal*, vol. 141, no. 1–3, pp. 112–118, 2008.

[4] Z.-X. Yang, Y. Chen, and Y. Liu, "Inclusion complexes of bisphenol A with cyclomaltoheptaose (β-cyclodextrin): solubilization and structure," *Carbohydrate Research*, vol. 343, no. 14, pp. 2439–2442, 2008.

[5] Y. Dong, D. Wu, X. Chen, and Y. Lin, "Adsorption of bisphenol A from water by surfactant-modified zeolite," *Journal of Colloid and Interface Science*, vol. 348, no. 2, pp. 585–590, 2010.

[6] W. Guo, W. Hu, J. Pan et al., "Selective adsorption and separation of BPA from aqueous solution using novel molecularly imprinted polymers based on kaolinite/Fe_3O_4 composites," *Chemical Engineering Journal*, vol. 171, no. 2, pp. 603–611, 2011.

[7] W.-T. Tsai, H.-C. Hsu, T.-Y. Su, K.-Y. Lin, and C.-M. Lin, "Adsorption characteristics of bisphenol-A in aqueous solutions onto hydrophobic zeolite," *Journal of Colloid and Interface Science*, vol. 299, no. 2, pp. 513–519, 2006.

[8] Z. Li, M. A. Gondal, and Z. H. Yamani, "Preparation of magnetic separable $CoFe_2O_4$/PAC composite and the adsorption of bisphenol A from aqueous solution," *Journal of Saudi Chemical Society*, vol. 18, no. 3, pp. 208–213, 2014.

[9] G. Liu, J. Ma, X. Li, and Q. Qin, "Adsorption of bisphenol A from aqueous solution onto activated carbons with different modification treatments," *Journal of Hazardous Materials*, vol. 164, no. 2-3, pp. 1275–1280, 2009.

[10] E. Yiantzi, E. Psillakis, K. Tyrovola, and N. Kalogerakis, "Vortex-assisted liquid-liquid microextraction of octylphenol, nonylphenol and bisphenol-A," *Talanta*, vol. 80, no. 5, pp. 2057–2062, 2010.

[11] M. Gómez, G. Garralón, F. Plaza, R. Vílchez, E. Hontoria, and M. A. Gómez, "Rejection of endocrine disrupting compounds (bisphenol A, bisphenol F and triethyleneglycol dimethacrylate) by membrane technologies," *Desalination*, vol. 212, no. 1–3, pp. 79–91, 2007.

[12] Z. Peng, F. Wu, and N. Deng, "Photodegradation of bisphenol A in simulated lake water containing algae, humic acid and ferric ions," *Environmental Pollution*, vol. 144, no. 3, pp. 840–846, 2006.

[13] C. P. Silva, M. Otero, and V. Esteves, "Processes for the elimination of estrogenic steroid hormones from water: a review," *Environmental Pollution*, vol. 165, pp. 38–58, 2012.

[14] S. Barnabé, S. K. Brar, R. D. Tyagi, I. Beauchesne, and R. Y. Surampalli, "Pre-treatment and bioconversion of wastewater sludge to value-added products—fate of endocrine disrupting compounds," *Science of the Total Environment*, vol. 407, no. 5, pp. 1471–1488, 2009.

[15] N. Yeddou and A. Bensmaili, "Kinetic models for the sorption of dye from aqueous solution by clay-wood sawdust mixture," *Desalination*, vol. 185, no. 1–3, pp. 499–508, 2005.

[16] I. Ali, M. Asim, and T. A. Khan, "Low cost adsorbents for the removal of organic pollutants from wastewater," *Journal of Environmental Management*, vol. 113, pp. 170–183, 2012.

[17] Y. P. Chin, S. Mohamad, and M. R. B. Abas, "Removal of parabens from aqueous solution using β-Cyclodextrin cross-linked polymer," *International Journal of Molecular Sciences*, vol. 11, no. 9, pp. 3459–3471, 2010.

[18] M. Kitaoka and K. Hayashi, "Adsorption of bisphenol A by cross-linked β-cyclodextrin polymer," *Journal of Inclusion Phenomena*, vol. 44, no. 1–4, pp. 429–431, 2002.

[19] H. Yamasaki, Y. Makihata, and K. Fukunaga, "Efficient phenol removal of wastewater from phenolic resin plants using crosslinked cyclodextrin particles," *Journal of Chemical Technology & Biotechnology*, vol. 81, no. 7, pp. 1271–1276, 2006.

[20] R. W. M. Krause, B. B. Mamba, L. N. Dlamini, and S. H. Durbach, "Fe-Ni nanoparticles supported on carbon nanotube-co-cyclodextrin polyurethanes for the removal of trichloroethylene in water," *Journal of Nanoparticle Research*, vol. 12, no. 2, pp. 449–456, 2010.

[21] P. Ayala, R. Arenal, M. Rümmeli, A. Rubio, and T. Pichler, "The doping of carbon nanotubes with nitrogen and their potential applications," *Carbon*, vol. 48, no. 3, pp. 575–586, 2010.

[22] S. Klimkova, M. Cernik, L. Lacinova, J. Filip, D. Jancik, and R. Zboril, "Zero-valent iron nanoparticles in treatment of acid mine water from in situ uranium leaching," *Chemosphere*, vol. 82, no. 8, pp. 1178–1184, 2011.

[23] S. Qi and L. C. Schideman, "An overall isotherm for activated carbon adsorption of dissolved natural organic matter in water," *Water Research*, vol. 42, no. 13, pp. 3353–3360, 2008.

[24] Y. S. Ho and G. McKay, "Pseudo-second order model for sorption processes," *Process Biochemistry*, vol. 34, no. 5, pp. 451–465, 1999.

[25] D. H. Lataye, I. M. Mishra, and I. D. Mall, "Adsorption of 2-picoline onto bagasse fly ash from aqueous solution," *Chemical Engineering Journal*, vol. 138, no. 1–3, pp. 35–46, 2008.

[26] W. Plazinski, W. Rudzinski, and A. Plazinska, "Theoretical models of sorption kinetics including a surface reaction mechanism: a review," *Advances in Colloid and Interface Science*, vol. 152, no. 1-2, pp. 2–13, 2009.

[27] K. Y. Foo and B. H. Hameed, "Insights into the modeling of adsorption isotherm systems," *Chemical Engineering Journal*, vol. 156, no. 1, pp. 2–10, 2010.

[28] Y. Ju-Nam and J. R. Lead, "Manufactured nanoparticles: an overview of their chemistry, interactions and potential environmental implications," *Science of the Total Environment*, vol. 400, no. 1–3, pp. 396–414, 2008.

[29] M. N. Timofeeff, T. K. Lowenstein, and W. H. Blackburn, "ESEM-EDS: an improved technique for major element chemical analysis of fluid inclusions," *Chemical Geology*, vol. 164, no. 3-4, pp. 171–181, 2000.

[30] Y.-M. Zheng, S.-F. Lim, and J. P. Chen, "Preparation and characterization of zirconium-based magnetic sorbent for arsenate removal," *Journal of Colloid and Interface Science*, vol. 338, no. 1, pp. 22–29, 2009.

[31] S. Akgöl and A. Denizli, "Novel metal-chelate affinity sorbents for reversible use in catalase adsorption," *Journal of Molecular Catalysis B: Enzymatic*, vol. 28, no. 1, pp. 7–14, 2004.

[32] G. Annadurai, L. Y. Ling, and J.-F. Lee, "Adsorption of reactive dye from an aqueous solution by chitosan: isotherm, kinetic and thermodynamic analysis," *Journal of Hazardous Materials*, vol. 152, no. 1, pp. 337–346, 2008.

[33] S. D. Mhlanga, S. P. Masinga, M. F. Bambo, B. B. Mamba, and E. N. Nxumalo, "A facile procedure to synthesize a three-component β-cyclodextrin polyurethane nanocomposite matrix containing Ag decorated N-CNTs for water treatment," *Nanoscience and Nanotechnology Letters*, vol. 5, no. 3, pp. 341–348, 2013.

[34] N. Savage and M. S. Diallo, "Nanomaterials and water purification: opportunities and challenges," *Journal of Nanoparticle Research*, vol. 7, no. 4-5, pp. 331–342, 2005.

[35] T. J. Malefetse, B. B. Mamba, R. W. Krause, and M. M. Mahlambi, "Cyclodextrin-ionic liquid polyurethanes for application in drinking water treatment," *Water SA*, vol. 35, no. 5, pp. 729–734, 2009.

[36] K. L. Salipira, R. W. Krause, B. B. Mamba, T. J. Malefetse, L. M. Cele, and S. H. Durbach, "Cyclodextrin polyurethanes polymerized with multi-walled carbon nanotubes: synthesis and characterization," *Materials Chemistry and Physics*, vol. 111, no. 2-3, pp. 218–224, 2008.

[37] K. L. Salipira, B. B. Mamba, R. W. Krause, T. J. Malefetse, and S. H. Durbach, "Carbon nanotubes and cyclodextrin polymers for removing organic pollutants from water," *Environmental Chemistry Letters*, vol. 5, no. 1, pp. 13–17, 2007.

[38] W.-T. Tsai, C.-W. Lai, and T.-Y. Su, "Adsorption of bisphenol-A from aqueous solution onto minerals and carbon adsorbents," *Journal of Hazardous Materials*, vol. 134, no. 1–3, pp. 169–175, 2006.

[39] J. Pan, X. Zou, X. Wang, W. Guan, Y. Yan, and J. Han, "Selective recognition of 2,4-dichlorophenol from aqueous solution by uniformly sized molecularly imprinted microspheres with β-cyclodextrin/attapulgite composites as support," *Chemical Engineering Journal*, vol. 162, no. 3, pp. 910–918, 2010.

[40] J. Lin and L. Wang, "Comparison between linear and non-linear forms of pseudo-first-order and pseudo-second-order adsorption kinetic models for the removal of methylene blue by activated carbon," *Frontiers of Environmental Science and Engineering in China*, vol. 3, no. 3, pp. 320–324, 2009.

[41] A. Gürses, Ç. Doğar, M. Yalçin, M. Açikyildiz, R. Bayrak, and S. Karaca, "The adsorption kinetics of the cationic dye, methylene blue, onto clay," *Journal of Hazardous Materials*, vol. 131, no. 1–3, pp. 217–228, 2006.

[42] Y.-S. Ho, C.-C. Chiang, and Y.-C. Hsu, "Sorption kinetics for dye removal from aqueous solution using activated clay," *Separation Science and Technology*, vol. 36, no. 11, pp. 2473–2488, 2001.

[43] M. Bhaumik, T. Y. Leswifi, A. Maity, V. V. Srinivasu, and M. S. Onyango, "Removal of fluoride from aqueous solution by polypyrrole/Fe_3O_4 magnetic nanocomposite," *Journal of Hazardous Materials*, vol. 186, no. 1, pp. 150–159, 2011.

[44] D. G. Myszka, "Kinetic, equilibrium, and thermodynamic analysis of macromolecular interactions with BIACORE," in *Methods in Enzymology*, G. K. A. Michael and L. Johnson, Eds., pp. 325–340, Academic Press, 2000.

[45] I. I. Fasfous, E. S. Radwan, and J. N. Dawoud, "Kinetics, equilibrium and thermodynamics of the sorption of tetrabromobisphenol A on multiwalled carbon nanotubes," *Applied Surface Science*, vol. 256, no. 23, pp. 7246–7252, 2010.